

Giant Magnetoresistive (GMR) Sensor Microelectromechanical System (MEMS) Device for Nondestructive Evaluation (NDE) Health Monitoring Applications for International Space Station (ISS)

R. Ramesham*, J. D. Olivas¹, S. Stokes², W. Wilson², and Edward Generazio³

*Jet Propulsion Laboratory, California Institute of Technology
4800 Oak Grove Drive, Pasadena, CA 91109

¹Lyndon B. Johnson Space Center, 2101 NASA Road 1, Houston, TX 77058

²Rice University, Houston, TX 77005

³Langley Research Center, Hampton, VA 23681-2199

ABSTRACT

With the imminent launch of the first International Space Station modules, NASA Office of Safety and Mission Assurance, specifically the Code Q Nondestructive Evaluation Program, is addressing issues of on-orbit station structural health monitoring. As part of this effort, Jet Propulsion Laboratory is working with NASA's Langley Research Center on development of novel devices and sensors for an NDE tool kit intended to be used by Space Station Astronauts for non-intrusive structural health assessment. JPL is currently investigating applicability of giant magnetoresistive technology, originally developed for high-density magnetic media, married to state of the art microelectromechanical systems (MEMS) for application as an acoustic sensor. In addition to space applications, these devices would have wide spread applicability in earthbound environments such as continuous/intermittent health monitoring of aircraft, hazardous process machinery and many other applications.

This paper discusses the fabrication aspects of a sensor device that is based on a sputter deposited, multilayer, giant magnetoresistive field sensor. The device consists of a micromachined microstructure (membrane, cantilever beam, bridge) and a sputtered hard magnetic film. The device detects acceleration by sensing changes in magnetic field caused by the displacement of the hard magnetic film on the microstructure. Utilizing the bulk micromachining approach, very thin (0.5 – 1 μm) silicon and silicon nitride membranes are fabricated by means of anisotropic etching of silicon wafers and/or reactive ion etching of silicon on insulator (SOI) or Low Pressure Chemical Vapor Deposited (LPCVD) silicon nitride films over silicon substrate. The primary objective of our program is to study spin valve structures (giant magnetoresistance in magnetic multilayers) and microelectronics fabrication issues in devices that exhibit the large magnetoresistive effect. A reliable GMR/MEMS device should have the following characteristics; a significant percentage change in resistance, high field resistance, low resistance noise, and a high bandwidth. These characteristics are very sensitive to the thickness of the various layers in device multilayers, the composition and microstructure of the individual layers. The eventual goal of our project is to optimize the giant magnetoresistive behavior of the device using a design of materials approach. Deposition and patterning of hard magnetic film over the microstructure and the bonding of microstructure over the GMR element are

discussed. We also present the fabrication and reliability issues associated with GMR devices.

Introduction

The measurement of acceleration has been accomplished using several technologies in high-reliability applications such as guidance control, detonation, and shock and vibration measurement. Electromechanical, piezoelectric, piezoresistive, and capacitive acceleration sensors are available and the literature pertinent to giant magnetoresistive sensors for the above applications are scanty. All accelerometers require the conversion of acceleration into a force, causing a displacement, which is then turned into an electrical signal. This displacement is resisted by a calibrated spring of some kind.

$$\begin{array}{ll} F = ma & 1 \\ F = -kx & 2 \\ a = -kx/m & 3 \end{array}$$

Where F = force, m = Mass, a = Acceleration, k = spring constant, and x = displacement. Equations describing accelerometers are simple and well known. Accelerometers measure “ a ” by knowing “ k ” and “ m ”, observing “ x ” and using equation 3 above.

The GMR effect was discovered in perfect-crystal samples exposed to very high fields.[1] The giant magneto resistive effect was recently discovered in sputtered metallic thin films consisting of magnetic layers a few nanometers thick separated by equally thin nonmagnetic layers. Large decrease in the resistance of these films is observed when a magnetic field is applied. The cause of this effect is the spin dependence of electron scattering and the spin polarization of conduction electrons in ferromagnetic metals. With layers of the proper thickness, adjacent magnetic layers couple antiferromagnetically to each other with the magnetic moments of each magnetic layer aligned antiparallel to the adjacent magnetic layers. Conduction of electrons, spin polarized in one magnetic layer with antiparallel conduction electron spins. Frequent scattering of electrons results in high electrical resistivity of the GMR device. If an external field overcomes the antiferromagnetic coupling it achieves parallel alignment of moments in adjacent ferromagnetic layers; the spin dependent scattering of conduction electrons is decreased and resistivity decreases. The size of this decrease in resistivity can be 10% to 20% and higher in GMR materials with multiple nonmagnetic layers.[2,3]

The primary advantage of GMR materials is greater sensitivity to magnetic fields. This increased sensitivity makes it possible to detect smaller change in the magnetic fields. Large signals from GMR materials structures also help overcome electronic noise. The difference between magnetoresistive (MR) and GMR sensors is sensitivity, measured by percent change in resistance. In a MR sensor a resistance change is caused by the intrinsic property of the sensing layer. In a GMR sensor a resistance change is caused by the quantum nature of electrons. [2-4]

Issues relating to GMR sensor fabrication: Controlling the thickness of the copper spacer layer, temperature stability, electrostatic discharge, change in magnetization, lift off technique approach, annealing of hard magnetic thin film, and the field damage will influence the GMR characteristics.[5] Issues associated with the reliability of GMR sensors are thickness control of the copper spacer layer. The other critical issue is the temperature stability. The production of spin valves uses an IrPtMn antiferromagnetic layer as a pinning layer for the spin valves. This layer can withstand cycling above 350°C. Cobalt and copper do not mix at moderate temperatures, however permalloy and copper do mix and if permalloy is used adjacent to copper, the spin valve will degrade around 200°C. GMR layers are extremely thin, only about 300 – 400 Å, so the temperature rise from a voltage spike can melt the layers. There is also danger of the magnetization changing if the temperature of the layer exceeds the Neel temperature of the antiferromagnetic layer. The GMR material should have resistance to electrostatic discharge and resistance to thermal degradation. The GMR element may be characterized by its change in resistance $\Delta R/R$ when the field changes by an amount of ΔH . The ratio of $\Delta R/\Delta H$ may be in the range of 0.1 Ω /Oersted. The objective in making this device is to measure to a typical distance, which is in the order of 1 nm. The sensitivity and response time of the mechanical assembly will depend on the coupling between the membrane (moving microstructure) and the GMR element. The maximum response time will be in the range of 10 – 0.2 μ sec for 1 nm displacement of moving part. A dogbone structure has been used to fabricate magnetoresistive GMR element that has a resistance, R that depends on the local field, H at the GMR sensor. If the resistance is used to measure field intensity the displacement “ d ” may be determined with a simple inversion of the function H as described in eqn. 4. [6-8]

Fabrication of GMR sensor: The fabrication of GMR sensor involves three steps and they are as follows: 1. Fabrication of GMR sensor on the substrate, 2. Fabrication of the movable microstructure such as a membrane or a cantilever beam, or a bridge and finally, 3. Deposition of hard magnetic thin film on the movable microstructure. Critical issues associated with the fabrication of a GMR sensor device are signal to noise ratio, geometry and lithographic definition of the spin valve on the substrate, magnetic properties of hard magnetic thin film, and process integration with surface and bulk micromachining processes.[9]

Patterning of spin valve: The GMR element may be fabricated using several layers of various metallic thin films patterned by using photolithography. Patterning of GMR element can be achieved by hydrochloric acid plasma, lift-off technique, ion milling, or chemical etching. Chemical etching may not yield fruitful results of patterning since the GMR element consists of various multi layers that could form galvanic couples in the chemical solutions. Different layers can be etched at different rates in the chemical etching solutions due to the galvanic coupling. We have used a single step self-aligned photolithographic lift-off technique to attain the patterning of GMR elements in this study. There may be some technical problems associated with the poor edge definition of GMR

elements in the lift-off technique. Therefore, experiments using HCl plasma and Ion milling will be planned shortly to attain GMR element fabrication.[10]

Possible hard magnetic thin film materials: A hard magnetic thin film element will be deposited over the moving microstructure (membrane, cantilever beam, or a bridge) and patterned using an appropriate technique. The lift-off technique may be used to pattern the hard magnetic thin film. Adhesion will be improved by depositing Cr by magnetron sputtering. Co-sputtering of CoCrTaPt will be deposited by lift-off technique. There is no wet etching solution available to pattern CoCrTaPt, FePt, CoPt to act as a hard magnetic thin film.[6]

Fabrication of moving microstructure: A moving microstructure of silicon, silicon nitride, or silicon dioxide may be fabricated using various approaches. A silicon membrane may be fabricated using anisotropic etching of silicon using silicon nitride mask and a potassium hydroxide solution. It is very difficult to fabricate a silicon membrane of 1 μm or less using this chemical etching solution approach. A silicon membrane may also be fabricated using a plasma-etching approach. Deep reactive ion etching technique has been used to etch the silicon substrate at a rate of 5 – 10 $\mu\text{m}/\text{min}$. Aluminum can be used as a mask to fabricate silicon membranes. It has been observed in our study that there will be a micromasking effect with aluminum in the RIE etched area. Thick photoresist has been used as a mask to etch silicon by RIE to fabricate silicon membranes.[11-13] It is difficult to fabricate 1 μm or less thick silicon membranes by RIE since the etching rate is significantly high. Therefore, an alternative approach could be silicon on insulator (SOI) substrate to fabricate silicon membranes. One may etch silicon either by RIE or chemical etching solutions. It is possible to fabricate 3 -5 μm thick silicon membranes. However, we need 1 μm or less thick silicon membranes to use as a moving microstructure to implement in the GMR sensor device. Finally, we have chosen to fabricate a silicon nitride membrane, which is apparently quite stable in KOH solutions. Silicon nitride has been grown on both sides of a silicon substrate using low-pressure chemical vapor deposition (LPCVD). The Si_3N_4 was patterned and then plasma etched down to the silicon substrate. The silicon substrate was etched in KOH solution until the other silicon nitride is reached. Thus 0.5 μm silicon nitride membranes are fabricated over silicon substrates.

Results and Discussion

Figure 1 shows the schematic of the complete giant magneto resistive (GMR) accelerometer device. This complete device may be fabricated over two silicon chips and finally may be bonded by an appropriate technique. A silicon substrate has been chosen in this study and silicon nitride was deposited using LPCVD technique. One side of the silicon substrate/silicon nitride was completely etched utilizing either plasma etch or hot phosphoric acid etch solution, while protecting the silicon nitride on the other side of the silicon substrate. Thermally grown silicon dioxide may be grown on the silicon substrate where silicon nitride was etched. The oxide is patterned and etched in the buffered oxide etch (BOE). The hard magnetic thin film was deposited and patterned over the moving microstructure. Silicon nitride on the other side of silicon substrate was patterned and

plasma etched down to the silicon substrate. The hard magnetic thin film was protected and (anisotropy) chemically etched silicon substrate all the way until the silicon nitride thin film. This has produced the moving microstructure with a hard magnetic thin film pattern. Another silicon substrate may be chosen and the growth of silicon dioxide was performed by thermal oxidation. Giant magneto resistive element will be fabricated using lift off technique on the silicon dioxide. These two chips will be bonded using anodic bonding or any other appropriate technique to assemble the device as shown in the Fig. 1. [14]

Figure 2 shows a scanning electron micrograph of the anisotropically etched silicon membrane. LPCVD silicon nitride has been used as a mask to etch silicon substrate and subsequently to fabricate the silicon membrane. This approach seems to be difficult to fabricate a silicon membrane of 1 μm or less thick. We have successfully fabricated a 0.5 μm LPCVD silicon nitride membrane to fabricate the eventual device as shown in the Fig. 1.

Figure 3 shows the schematic diagram of the GMR element fabrication. A silicon substrate has been chosen and oxidized by thermal oxidation. The photoresist was spin coated and patterned using photolithography. Tantalum was deposited for electrical contact and to isolate the permalloy from the silicon dioxide. A sensing layer of permalloy was deposited and subsequently cobalt, copper, cobalt, iron-manganese, and finally tantalum were deposited in the same deposition set-up using the same vacuum chamber. Cobalt was deposited to separate the mixing of permalloy and copper and also the mixing of iron-manganese and copper. Copper is deposited to act as a spacer in this device. The top tantalum layer is deposited to protect the device from oxidation and contamination with other impurities. [14-17]

Figure 4a shows the scanning electron micrograph of the fabricated GMR device over the silicon dioxide/silicon substrate using lift-off technique. Figure 4b and 4c are the magnified views of the single GMR element and a corner of the GMR element. Figure 5a-f show the scanning electron micrographs of the GMR element in various regions of the device. The lift-off technique employed in this experiment has yielded poor edge definition. We feel that, this might effect the anticipated sensor response results.

During the growth of GMR stack, a magnetic field is applied to the sample to induce easy and hard axes in the magnetic layers and set the direction for the pinning field in the antiferromagnetic layer. In operation the magnetic field to be sensed is applied parallel to the hard axis since there is very little hysteresis along this direction and the response is linear for small changes in field. Figure 6 is a plot of the resistance change versus the field applied along the hard axis. The resistance changed by about 3.9 % over the entire field range. There are some issues with the liftoff that lead to a less than ideal GMR curve in Figure 6. Specifically, any surface contamination left after the development of the photoresist will result in rough layers. Rough or wavy interfaces in GMR device increases the ferromagnetic coupling between the two magnetic layers. Also, if the walls of the resist were not perfect additional magnetic coupling could arise.

Figure 7 shows the power versus the frequency when an ac field was applied to the GMR device along with a dc bias field of 15 Oe. The magnitude of the field applied in Fig. 7 was 0.6 Oe (500 Hz sine wave) and the current through the device was 6 mA (device resistance is about 480 K). The absence of higher harmonic peaks indicates that there was little distortion and an output of pure sine wave. The baseline noise in Fig. 7 is due to intrinsic 1/f noise in the spin valve. 1/f noise is the dominant noise source until about 20 KHz depending on the current, at higher frequencies thermal noise is dominant. The magnitude of the 1/f noise increases as the square of the current.

Table 1 shows the some of the experimental spin valve configurations that have been tested in the laboratory at Rice University. Adding the cobalt layer in the GMR device structure has significantly improved the device characteristics. Further experiments are underway to understand the significance of the various layers.

Table 1: The change in resistance as a function of spin valve configuration [16]

Device #	Spin Valve Configuration	$\Delta R/R$	Oe
1	Co/Cu/Co/FeMn	9.9%	0.81
2	NiFe/Cu/NiFe/FeMn	4.3%	1.51
3	NiFe/Co/Cu/Co/NiFe/FeMn	9.1%	--

Table 2 shows the test results on the some of the GMR devices fabricated at the Rice University. The change in resistance was high (6.3%) when there is thick cobalt layer and also the permalloy layer was absent. A permalloy layer has been incorporated in the device 2 and cobalt layer thickness layer has been reduced to 15 Å. The change in resistance has reduced to 4.5%. The cobalt layer has been completely eliminated in the device 3 and the change in resistance has been reduced further. The copper layer thickness is different from the critical thickness required to obtain high change in resistance. Further experiments are underway to characterize the GMR devices.

Table 2: GMR Device Test Results

Device #	Ta (Å)	Py (Å)	Co (Å)	Cu (Å)	Co (Å)	Py (Å)	FeMn (Å)	Ta (Å)	$\Delta R/R$
1	64	--	50	44	50	--	80	64	6.3%
2	50	50	15	44	15	50	80	50	4.5%
3	50	50	--	44	--	50	80	50	1.6%

Conclusions

We have used the appropriate layers such as sensing layer, conducting spacer and antiferromagnetic layer and other space layers to avoid the mixing of the sensing layer and

conducting spacer. Identified the problems associated with the fabrication of very thin silicon membranes and we have fabricated 0.5 micron low pressure chemical vapor deposited silicon nitride membranes using anisotropic chemical etching of silicon and plasma etching of silicon nitride. Identified the hard magnetic thin film, which will be deposited over the moving silicon nitride microstructure to demonstrate the GMR sensor device. We will shortly be assembling the GMR devices, hard magnetic thin film fabricated over moving silicon nitride microstructure components using, and appropriate process to characterize the sensor response characteristics.

Acknowledgments

This research work was carried out at the Jet Propulsion Laboratory, California Institute of Technology and Rice University and was supported by NASA. Thanks are due to Mr. Stephen R. Bolin for his constructive comments on the manuscript.

References

1. M. N. Baibich, J.M. Broto, A. Fert, F. Nguyen Van Dau, F. Petroff, P. Etienne, G. Creuzet, A. Friederich, and J. Chazelas, *Phys. Rev. Lett.*, 61 (1988) 2472.
2. S.P. Parkin, "Giant Magnetoresistance in sputtered magnetic superlattices", 35th Annual conference on magnetism and magnetic materials, November 27 – December 4, 1989. Abstract was published in *Journal of Applied Physics*, 67, 5931 (1990).
3. Nonvolatile Electronics Inc., Engineering & Application Notes, <http://www.nve.com>.
4. P. Grunberg, "Magnetic field sensor with ferromagnetic thin film layers having magnetically antiparallel polarized components," U.S. Patent, 4,949,039.
5. B. A. Gurney, V.S. Speriosu, D.R. Wilhoit, H. Lefakis, R.E. Fontana, Jr., "Can spin valve be reliably deposited for magnetic recording?", *J. Appl. Phys.*, 81 (1997) 3998.
6. S. Mao, N. Amin, and E. Murdock, *J. Appl. Phys.*, 83 (1998) 6807.
7. A. Wallash, *Data Storage, Test and Measurement*, January 1998, p. 37.
8. J. Szucs, T. O'Brien, and D.K. Lottis, S. Gangopadhyay, S. Mao, and E. Murdock, *J. Appl. Phys.*, 81 (1997) 4014.
9. R.J. M. van de Veerdonk, P.J. Belein, K.M. Schep, J.C.S. Kools, M.C. de Nooijer, M.A. Gijs, R. Coehoorn, W.J.M. de Jonge, *J. Appl. Phys.*, 82 (1997) 6152.
10. M. Xiao and M.H. Kryder, *Electrochemical Society Proceedings, Proceedings of the Fourth International Symposium on Magnetic Materials, processes and Devices*,

Application to storage and microelectromechanical systems (MEMS), Edited by L.T. Romankiw and D. A. Herman, Jr., Vol. 95-18, p. 51 (1995).

11. C. D. Ellis, Auburn University, Personal communication, Jan 1998.
12. R. Ramesham, C.D. Ellis, J.D. Olivas, and S. Bolin, Thin Solid Films, "Fabrication of diamond membranes for MEMS using reactive ion etching of silicon," Thin Solid Films, 1998. (In Press).
13. Marc Madou, Fundamentals of Microfabrication, CRC Press, New York, 1997.
14. W.F. Egelhoff, Jr., P.J. Chen, C.J. Powell, M.D. Stiles, R.D. McMichael, C.L. Lin, J.M. Sivertsen, J.H. Judy, K. Takano, A.E. Berkowitz, T.C. Anthony, and J.A. Brug, J. Appl. Phys., 79 (1996) 5277.
15. V.S. Speriosu, J.P. Nozieres, B.A. Gurney, B. Dieny, T.C. Huang, and H. Lefakis, Physical Review B, 47 (1993) 11579.
16. J.P. Nozieres, V.S. Speriosu, B.A. Gureny, B. Dieny, H. Lefakis, and T.C. Huang, J. Magnetism and Magnetic Materials, 121 (1993) 386.
- 17 B. Dieny, J. Magnetism and Magnetic Materials, 136 (1994) 335.

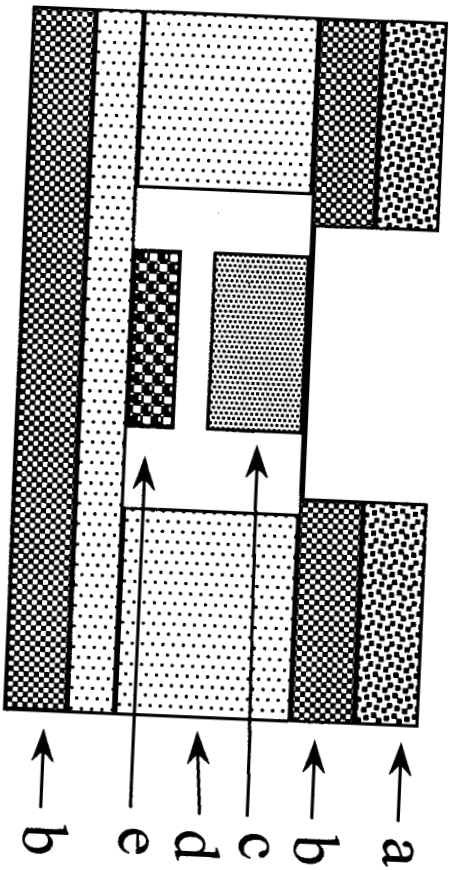


Figure 1: Schematic of the Complete Giant Magnetic Resistive (GMR) Accelerometer Device. a. Silicon nitride, b. Silicon, c. Hard magnetic thin film, d. Silicon dioxide, e. GMR Element.

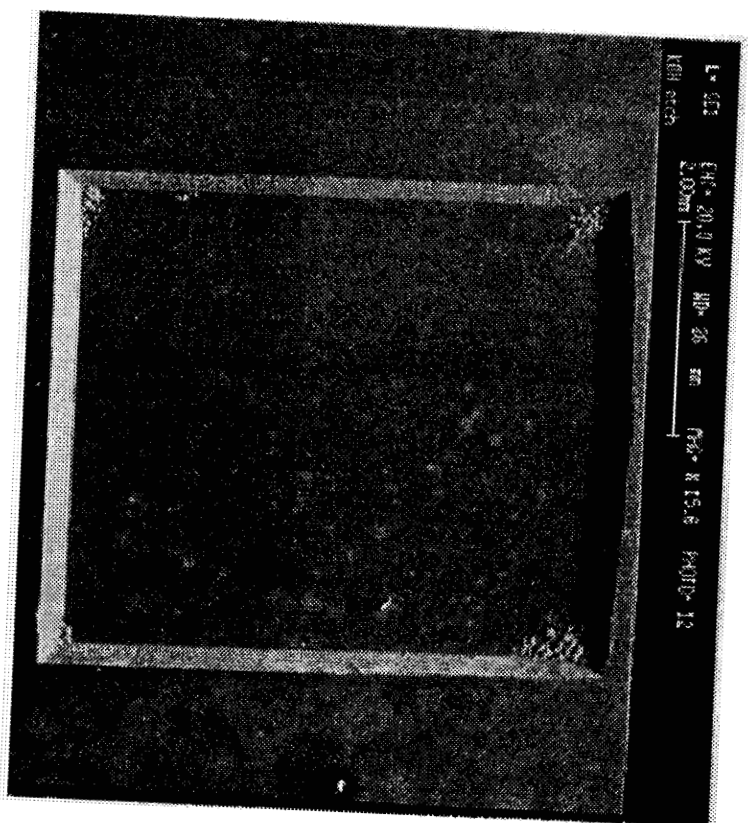


Figure 2 : Scanning electron micrograph of silicon membrane fabricated using anisotropic etching of silicon substrate.

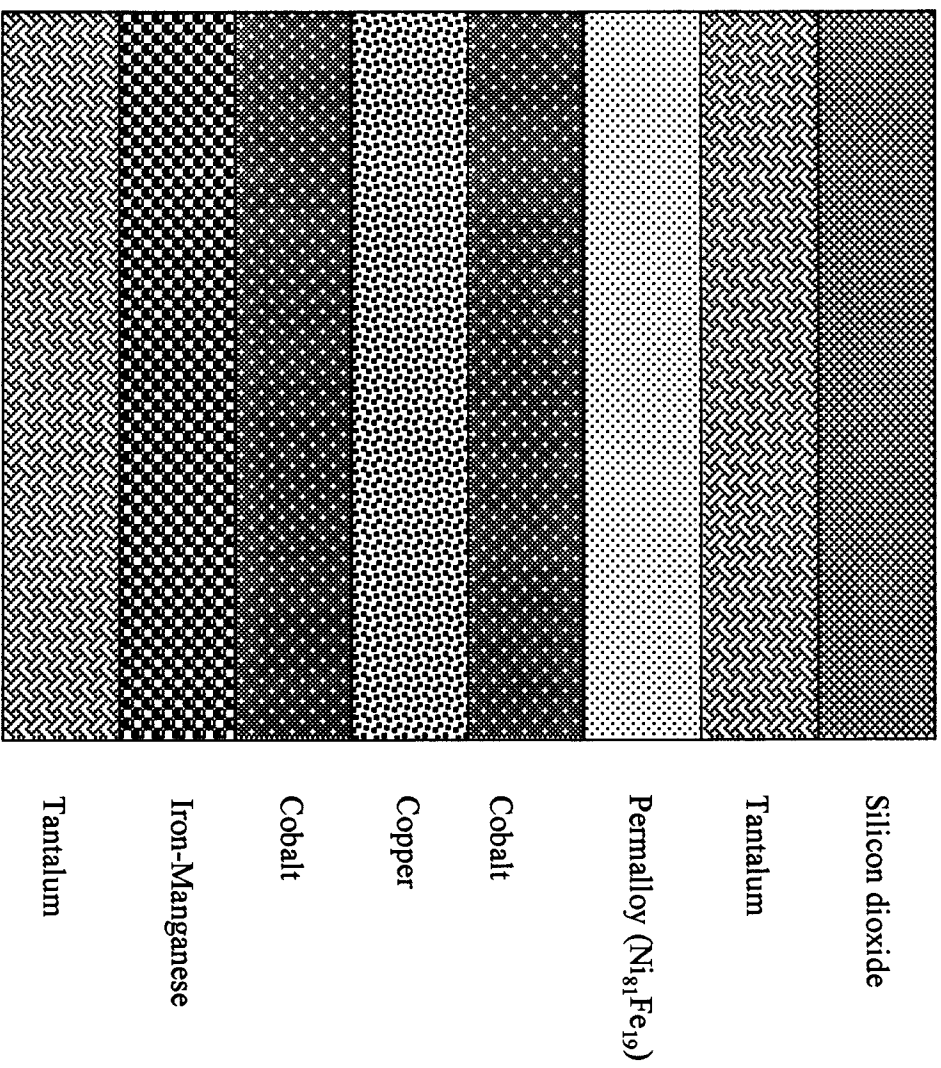


Figure 3: Schematic Diagram of GMR Element Fabrication

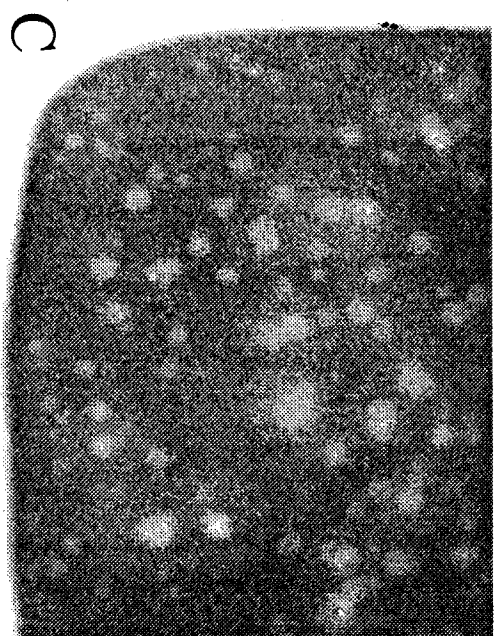
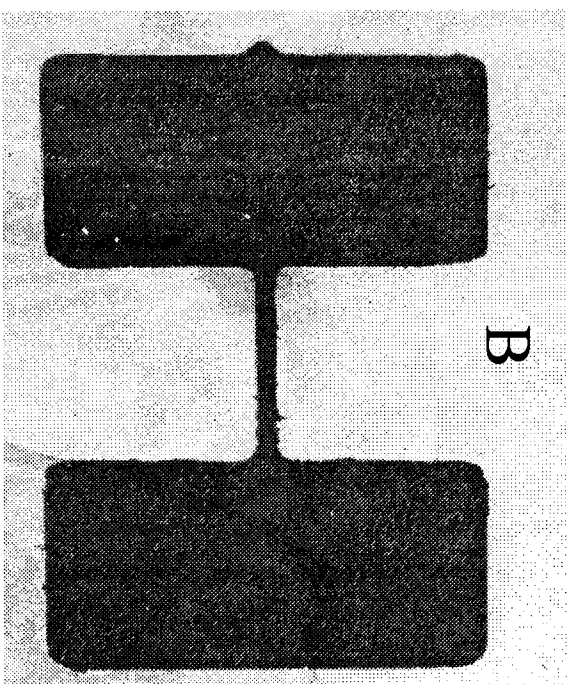
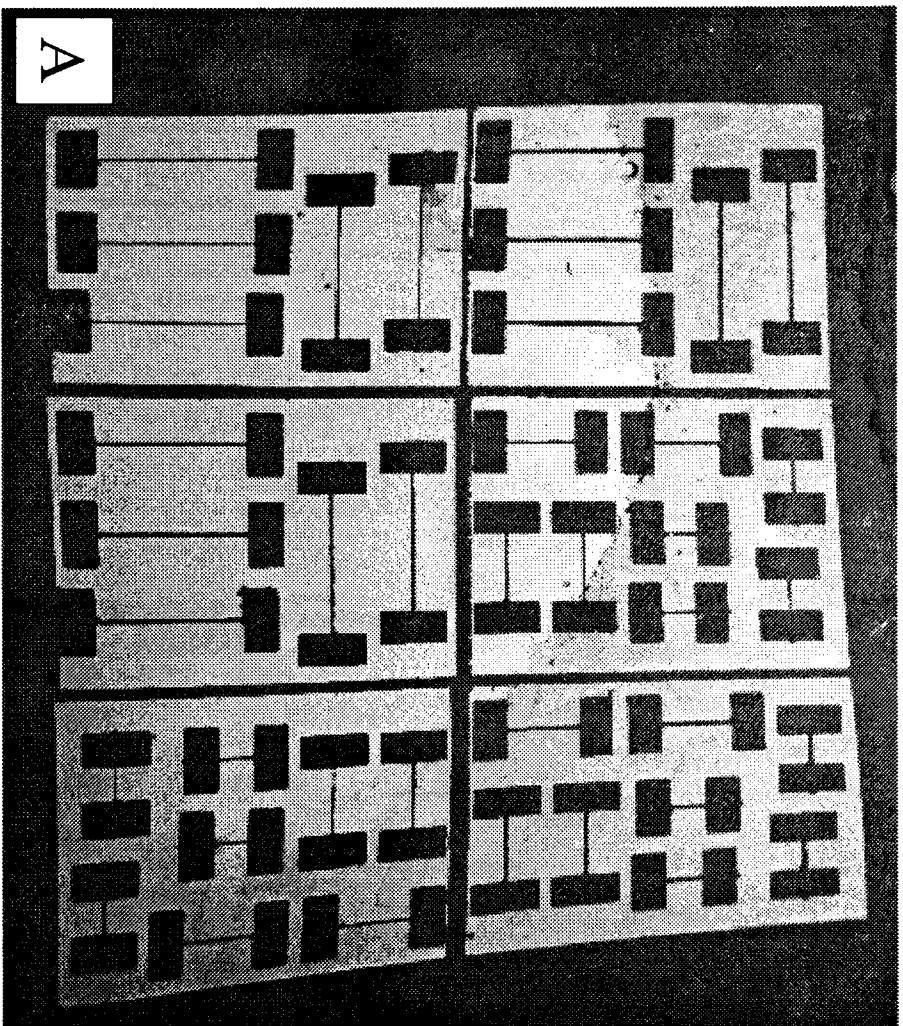


Figure 4 : Fabricated GMR Device (a) Complete device, (b) Single GMR Device, and (c) Magnified view of the corner of GMR device.

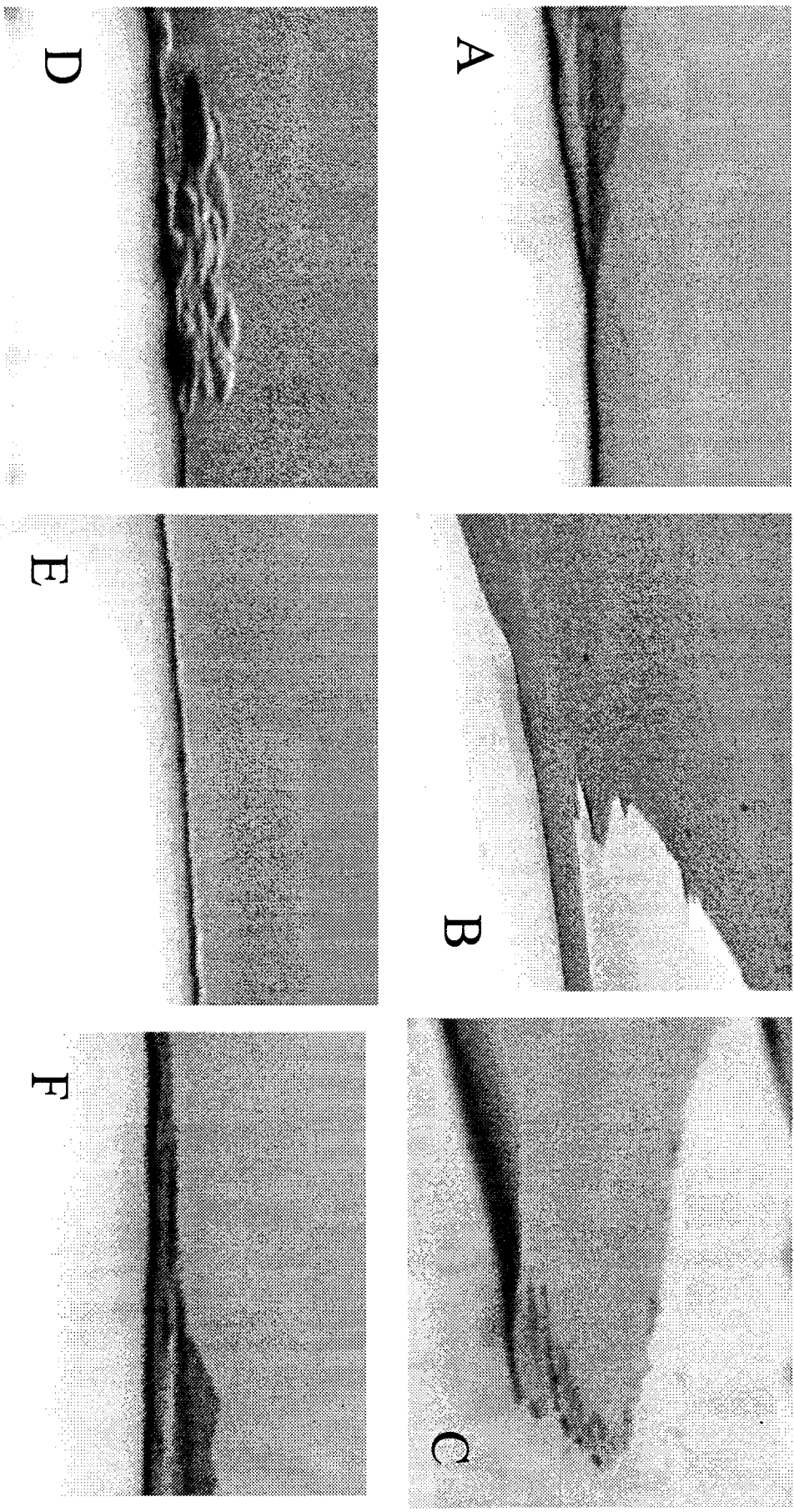


Figure 5: Scanning Electron Micrographs (a,b,c,d,e, and f) of the Fabricated GMR Device.

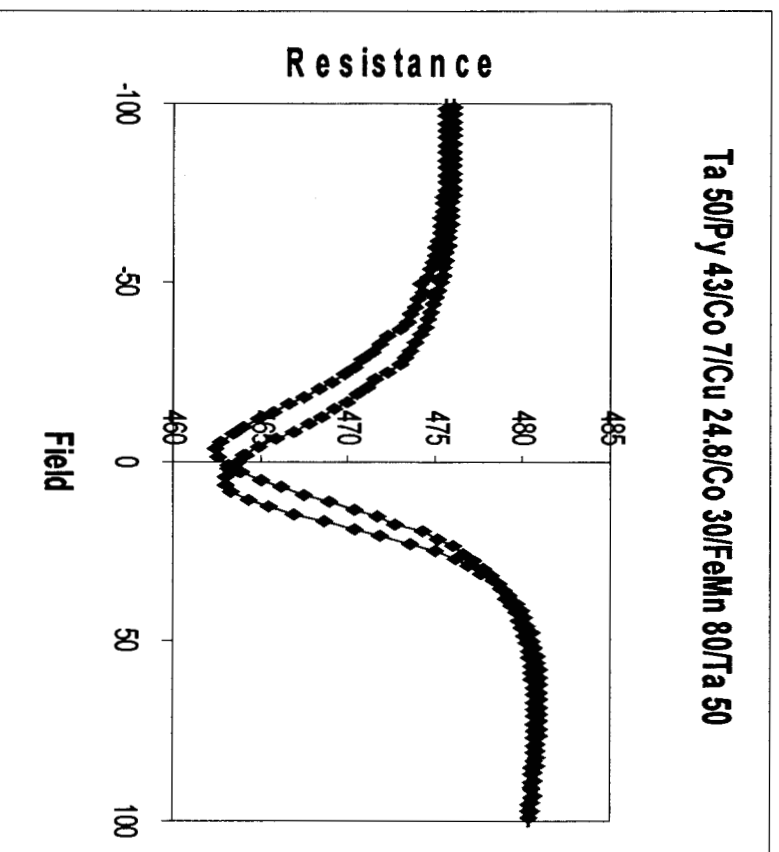


Figure 6: Resistance change in the GMR sensor device versus the applied field

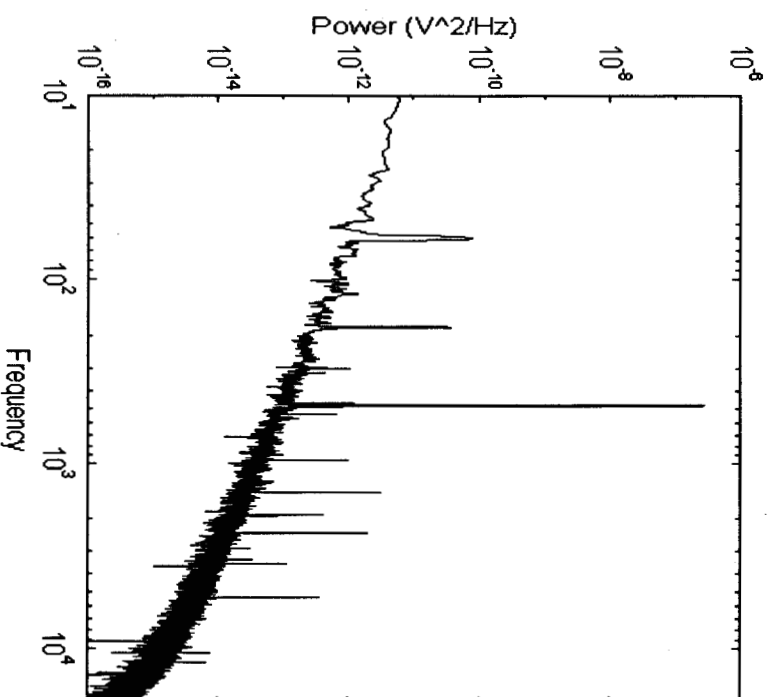


Figure 7: Power versus the frequency used to test the GMR sensor device